PHYSICAL REVIEW E **95**, 060103(R) (2017)

Columnar domains and anisotropic growth laws in dipolar systems

Arunkumar Bupathy,[1] Varsha Banerjee,[1] and Sanjay Puri[2]
[1]*Department of Physics, Indian Institute of Technology Delhi, New Delhi 110016, India*
[2]*School of Physical Sciences, Jawaharlal Nehru University, New Delhi 110067, India*
(Received 29 December 2016; published 28 June 2017)

Magnetic and dielectric solids are well-represented by the Ising model with dipolar interactions (IM+DI). The latter are long-ranged, fluctuating in sign, and anisotropic. Equilibrium studies have revealed novel consequences of these complicated interactions, but their effect on nonequilibrium behavior is not explored. We perform a deep temperature quench to study the kinetics of domain growth in the $d = 3$ IM+DI. Our main observations are (i) the emergence of columnar domains along the z axis (Ising axis) with a transient periodicity in the xy plane; (ii) anisotropic growth laws: $\ell_\rho(t) \sim t^\phi$; $\ell_z(t) \sim t^\psi$, where $\vec{\rho} = (x, y)$ and ℓ is the characteristic length scale; (iii) generalized dynamical scaling for the correlation function: $C(\rho, z; t) = g(\rho/\ell_\rho, z/\ell_z)$; and (iv) an asymptotic Porod tail in the corresponding structure factor: $S(k_\rho, 0; t) \sim k_\rho^{-3}$; $S(0, k_z; t) \sim k_z^{-2}$. Our results explain the experimentally observed columnar morphologies in a wide range of dipolar systems, and they have important technological implications.

DOI: 10.1103/PhysRevE.95.060103

Many magnetic and dielectric solids involve long-range dipole-dipole interactions in addition to short-range exchange interactions [1–11]. The simplest model that describes them is the nearest-neighbor (NN) Ising model with dipolar interactions (IM+DI). For N Ising spins on a d-dimensional lattice, the Hamiltonian is given by

$$\mathcal{H} = -J \sum_{\langle i,j \rangle} \sigma_i \sigma_j - D \sum_{\substack{i,j \\ i \neq j}} \left(\frac{3\cos^2 \theta_{ij} - 1}{r_{ij}^3} \right) \sigma_i \sigma_j . \qquad (1)$$

Here $\sigma_i = \pm 1$, J and D (>0) are the strengths of NN exchange and dipolar interactions (DI), $\vec{r}_{ij}$ is the vector joining σ_i and σ_j in units of lattice spacing a, and θ_{ij} is the angle made by $\vec{r}_{ij}$ with the Ising axis (z axis). The presence of r_{ij}^3 in the denominator makes DI long-ranged due to which spin-spin interactions are significant up to many lattice spacings. The coupling is ferromagnetic for $55^\circ < \theta < 125^\circ$ and antiferromagnetic for other values. Therefore, a ferromagnetic alignment is favored along the z direction, but domain walls are preferred in the xy plane. Further, the conflicting interactions cause spin frustrations that introduce several local minima in the energy function.

The difficulties in handling long-ranged DI make the analysis of IM+DI challenging analytically and computationally. Consequently, there are very few studies of this model, although it is realized by a large number of complex materials. These isolated studies have addressed phases and critical points that reveal novel manifestations of DI and are summarized below: (i) Ground-state (GS) enumerations ($T = 0$) and Monte Carlo (MC) simulations ($T \neq 0$) for a cubic lattice (L^3, $L = 6,8$) indicate that the model exhibits distinct phases as the ratio $\Gamma = J/D$ is varied, e.g., $\Gamma < 0.13$ gives different antiferromagnetic structures while $\Gamma > 0.16$ yields a ferromagnet [1]. (ii) The GS of a slab $L \times L \times W$ ($L \gg W$), on the other hand, is comprised of parallel striped domains that transit to a *bubble phase* upon application of an external magnetic field [12]. (iii) Similarly, the GS of an elongated sample $W \times W \times L$ is ferromagnetic [13]. (iv) Using Feynman-graph expansions, Larkin and Khmel'nitskii demonstrated that the critical exponents for IM+DI in $d = 3$ are those of the classical Landau theory with logarithmic corrections to the power laws [14]. (v) These results were reconfirmed by Aharony using exact renormalization-group methods. He further showed that the model belongs to the same universality class as the short-range Ising ferromagnet in $(d + 1)$ dimensions [15]. (vi) Using a field-theoretic approach, Frey *et al.* [16] demonstrated that the model exhibits a crossover from Ising behavior with nonclassical exponents to an asymptotic uniaxial dipolar behavior characterized by classical exponents with logarithmic corrections. Later, Henneberger *et al.* also observed this crossover from mode-coupling theory [17]. (vii) These logarithmic corrections were then validated by experiments on uniaxial ferromagnets and ferroelectrics, confirming that they are physical realizations of IM+DI [7,18,19].

Surprisingly, there are no studies that address the nonequilibrium properties of the IM+DI in $d = 3$. There are a few in $d = 2$ [20,21], but they lack the anisotropy of the $d = 3$ model. How this anisotropy affects the dynamics is an open question. In this context, let us consider the kinetics of domain growth or phase ordering following a sudden quench in temperature. The dynamical process by which the system in the disordered phase evolves to an ordered phase by the formation of domains and their subsequent growth is called coarsening [22,23]. If the morphology of the coarsening domains is unchanged in time, the system exhibits dynamical scaling and is characterized by a unique length scale $\ell(t)$ that grows with time. The growth law reveals details of the free-energy landscape and relaxation time-scales. For example, pure and isotropic systems with nonconserved kinetics such as the Ising model ($D = 0$) obey the Lifshitz-Allen-Cahn (LAC) law: $\ell(t) \sim t^{1/2}$ [24,25]. It is characteristic of systems with no energy barriers to coarsening and a unique relaxation time-scale. Systems with disorder and competing interactions, on the other hand, have a complicated free-energy landscape and a plethora of relaxation time-scales. The interfaces are rough fractals, and the barriers to coarsening $E_B \sim \ell^{2-\alpha}$, where α is the *roughness exponent* [26–28]. Domain growth in these systems exhibits logarithmic behavior in the asymptotic limit [29].

In this paper, we present a study of the kinetics of domain growth after a deep quench in the $d = 3$ IM+DI using MC simulations. We focus on the following issues: How are the anisotropy and competing nature of the interactions reflected in the growth law? Does this system still exhibit dynamical scaling? Are there signatures of spin frustrations, barriers to coarsening, and multiple relaxation time-scales? The answers to these questions have important implications for both equilibrium and nonequilibrium properties.

By using Ewald summation [30] to efficiently handle DI, we were able to simulate large systems of up to 128^3 spins. We perform deep quenches into the ferromagnetic phase, and we study domain growth at different values of Γ. The main results of our paper are as follows: (i) The anisotropy effects of DI are clearly manifested in our $d = 3$ simulations. Elongated columnar domains emerge along the z axis after the quench, and they grow rapidly to span the lattice length (along z). There is a transient signature of periodic arrangement of the coarsening columns in the xy plane. (ii) Domain growth is anisotropic in the xy plane and along z: $\ell_\rho(t) \sim t^\phi$, $\ell_z(t) \sim t^\psi$, where $\vec{\rho} = (x,y)$ and ℓ is the length scales. The exponents ϕ and ψ are *universal*. (iii) The correlation function exhibits generalized scaling: $C(\rho,z;t) = g(\rho/\ell_\rho, z/\ell_z)$. Correspondingly, the structure factor $S(k_\rho,k_z;t)$ is also anisotropic. (iv) The large-k behavior of $S(k_\rho,k_z;t)$ exhibits Porod decay: $S(k_\rho,0;t) \sim k_\rho^{-3}$; $S(0,k_z;t) \sim k_z^{-2}$. Thus the interfaces are smooth in spite of the anisotropy and competing DI.

There is a wide class of physical systems that are well represented by IM+DI. A thermal quench is easy to induce in a laboratory and is usually the starting point for nonequilibrium studies. Therefore, our results on phase ordering have great relevance to many experimental systems. These include nuclear magnetic moments in alkali hydrides and solid ^{3}He [2,3]; electron magnetic moments in rare-earth fluorides, chlorides, and hydroxides [4–6]; electric dipole moments in ferro and antiferroelectric structures [7–9]; etc. Another relevant system of current interest is the rare-earth compound $LiHoF_4$ and its dilution series $LiHo_xY_{1-x}F_4$. Apart from the wide variety of phases, they also exhibit a quantum phase transition upon application of a transverse field [10,11]. Our study will also be useful for understanding ordering phenomena in substitutional and interstitial alloys (where short-range chemical forces compete with long-range elastic forces), superionics, molecular crystals, adsorbed monolayers at surfaces, etc. [1]. Many experimental measurements in dipolar systems probably access nonequilibrium states with long relaxation times. We expect our study to improve interpretations of these observations.

We now describe the details of our simulations. Our starting point is a random configuration of $\sigma_i = \pm 1$ (disordered phase) quenched rapidly to $T = 0.25T_c$ in the ordered phase. To determine the temperature quenches, we use the phase diagram obtained by Kretschmer and Binder for a simple cubic lattice [1]. The quenches were performed only in the ferromagnetic phase, i.e., $\Gamma > 0.16$. The system evolves via Glauber spin-flip kinetics with METROPOLIS acceptance rates. All simulations were done on cubic lattices of size 128^3 unless stated otherwise. Each data set has been averaged over 48 different initial conditions. The standard error in a data point is smaller than the symbol size and is not shown for clarity. The Ewald summation technique (with metallic boundaries) was used to compute the dipolar term of Eq. (1), accurate up to an error $\delta < 10^{-3}$ [30]. From our simulations of smaller lattices with better error bounds ($\delta < 10^{-4}$), we found that a further increase in accuracy did not alter the growth laws. The system was allowed to evolve up to 1500 Monte Carlo steps (MCS), which took about 150 h per run on an Intel Xeon E5-2680 v3 CPU running at 2.5 GHz. Our large system size, Ewald sums, long evolution times, and significant averaging have been computationally challenging, but they enabled us to make accurate observations of nonequilibrium properties.

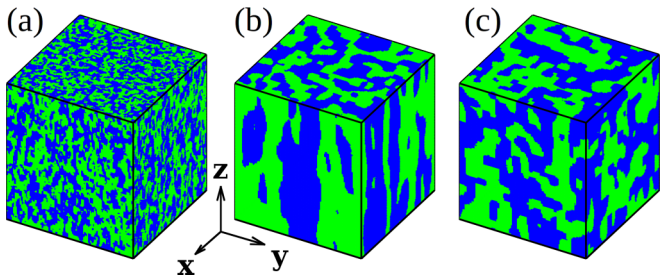

FIG. 1. Domain morphologies for different values of Γ and t (in MCS): (Γ, t) = (a) (10, 4), (b) (10, 64), and (c) (100, 64). Green (gray) and blue (black) represent $\sigma_i = 1$ and -1, respectively.

In Fig. 1, we show the snapshots of domain morphologies for different values of Γ and t (in MCS): (Γ, t) = (a) (10, 4), (b) (10, 64), and (c) (100, 64). Green (gray) and blue (black) regions represent $\sigma_i = 1$ and -1, respectively. Immediately after the quench [Fig. 1(a)], columnar domains start forming along the z direction and grow rapidly. In Fig. 1(b), the length of the domains is almost equal to the size of the simulation cell. Such elongated needlelike domain structures have been seen experimentally [31] as well as in MC simulations of the uniaxial dipolar magnet $LiHoF_4$ [10]. They are also observed in single crystals of $BaTiO_3$, rochelle salt, and KH_2PO_4 using optical techniques [9]. Recall that the dipolar interaction favors ferromagnetic alignment in the z direction and domain walls in the xy plane. The effect of dipolar strength can be seen from Figs. 1(b) and 1(c): for stronger DI ($\Gamma = 10$) the domains are highly anisotropic, while for weak DI ($\Gamma = 100$) they are more isotropic.

How do we quantify morphologies and domain growth? The usual probes are the correlation function $C(\vec{r},t)$ and the structure factor $S(\vec{k},t)$ [22]. If the domain growth is characterized by a unique length scale $\ell(t)$, then $C(\vec{r},t)$ and $S(\vec{k},t)$ show the dynamical scaling property: $C(\vec{r},t) = g(r/\ell)$; $S(\vec{k},t) = \ell^d f(k\ell)$. Because the morphologies are anisotropic, we introduce $C(\vec{r},t) \equiv C(\vec{\rho},z;t)$, where $\vec{\rho} = (x,y)$. If we assume that there are unique length scales ℓ_ρ and ℓ_z characterizing domain growth in the xy and z directions, then the correlation function should exhibit generalized dynamical scaling [32,33]: $C(\vec{\rho},z;t) = g(\rho/\ell_\rho, z/\ell_z)$. We designate $C(\vec{\rho},0;t) = g_1(\rho/\ell_\rho)$ and $C(0,z;t) = g_2(z/\ell_z)$. There are corresponding forms for $S(\vec{k},t) \equiv S(\vec{k_\rho},k_z;t)$, where $\vec{k_\rho} = (k_x,k_y)$.

In Fig. 2(a), we show the scaled correlation functions in the xy plane: $C(\vec{\rho},0;t)$ versus ρ/ℓ_ρ at t (MCS) = 16, 64, 256, and 1024 for $\Gamma = 10$. The corresponding scaled correlation

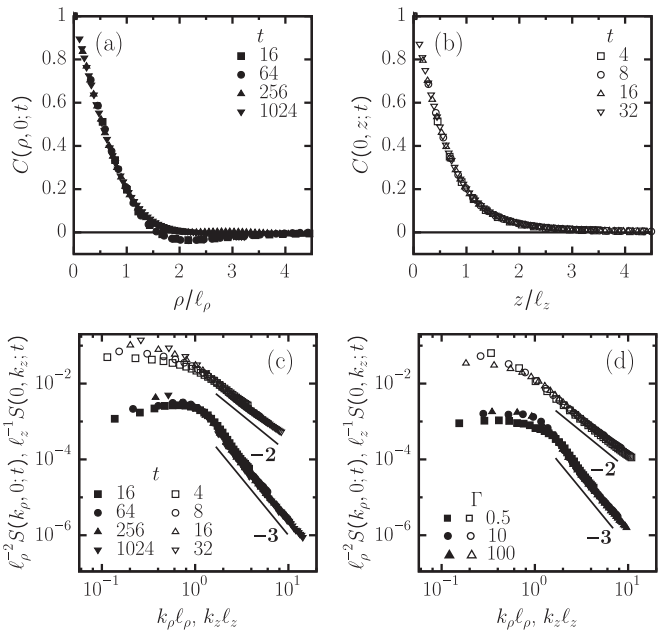

FIG. 2. Scaled correlation functions for $\Gamma = 10$ at different values of t (in MCS): (a) $C(\rho,0,t)$ vs ρ/ℓ_ρ (filled symbols); (b) $C(0,z,t)$ vs z/ℓ_z (open symbols). (c) Corresponding scaled structure factors indicating Porod decay (solid lines). (d) Analogous plot for $t = 32$ MCS and different values of Γ. The xy and z data sets are shifted vertically for clarity.

functions in the z direction, $C(0,z;t)$ versus z/ℓ_z, are shown in Fig. 2(b). The data for $t > 32$ are not shown here as the growth at these times is limited by the finite size of the simulation cell. Both data sets exhibit dynamical scaling, indicating that the system is characterized by unique but distinct length scales along the xy and z directions. Notice that $C(\rho,0;t)$ for $t \leqslant 64$ MCS shows oscillatory behavior characteristic of periodically modulated structures [22]. We have examined xy cross sections of the snapshots in Fig. 1(a). These show a bicontinuous morphology reminiscent of phase-separation kinetics rather than the bloblike morphology that characterizes nonconserved dynamics. In Fig. 2(c) we show the corresponding scaled structure factors on a log-log scale. The system exhibits the Porod law $S(k,t) \sim k^{-(d+1)}$ in both directions, indicating the presence of smooth interfaces. To probe the effect of DI, we plot in Fig. 2(d) the structure factor for $\Gamma = 0.5$, 10, and 100 at $t = 32$ MCS. The data collapse demonstrates that the morphologies are invariant with respect to Γ.

Next, we quantify the domain growth. In Fig. 3(a), we plot $\ell_\rho(t)$ (solid symbols) and $\ell_z(t)$ (open symbols) as a function of t on a log-log scale for $\Gamma = 0.5$, 10, and 100. For $\Gamma = \infty$ ($D = 0$), the growth is isotropic and governed by the LAC law with $\phi = \psi = 0.5$ (shown for reference). In the case of *isotropic* long-ranged interactions $\sim r^{-3}$, it was argued by Bray that $\psi = 1$ [34] (also shown for reference). The dipolar interactions in our model are *anisotropic*. Consequently, for $\Gamma = 0.5$ and 10, $\ell_z(t)$ grows faster than the LAC law ($\psi = 0.5$) but slower than Bray's prediction. For $\Gamma = 100$, $\psi \simeq 0.5$ as the dipolar strength is very small. On the other hand, ℓ_ρ obeys LAC growth with $\phi \simeq 0.5$. We also point out that log-log plots

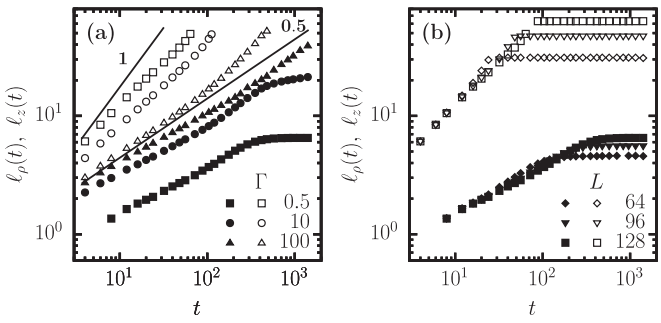

FIG. 3. (a) ℓ vs t in the xy plane (solid symbols) and the z direction (open symbols) for different values of Γ. Reference lines with slopes 1 and 1/2 are also indicated (see text). (b) Length scales for $\Gamma = 0.5$ and system sizes $L = 64,96,128$.

underestimate exponents due to the presence of a nonzero offset.

To study the system-size effects, we show ℓ_ρ and ℓ_z as a function of t for $\Gamma = 0.5$ and $L = 64$, 96, and 128 in Fig. 3(b). The growth exponents are unaffected by the system size L. Note that the flattening of ℓ_z at late times is observed after the vertical columns have coarsened to L. (It can be seen that ℓ_ρ also saturates soon thereafter.) Coarsening of domains then occurs only in the xy plane via lateral movement of (vertical) domain walls. The system typically settles into a near-equilibrium state with one domain wall in the z direction. As stated earlier, the stable equilibrium state is ferromagnetic for the parameter values considered here. It is interesting to note that diverse initial conditions yield nearly the same "ground state" of the system.

We emphasize that anisotropic interactions do not always give rise to anisotropic exponents. We have performed MC simulations of the NN IM with interactions J_ρ in the (x,y) plane and $J_z = 5J_\rho$ along the z direction, and we found that $\psi = \phi \simeq 1/2$. The anisotropic growth exponents in our dipolar system are a consequence of the complicated DI, which fluctuate in sign and are long-ranged.

Finally, we conclude this paper with a discussion on what our results could mean for experimentalists and theorists. The Ising model with dipolar interactions (IM+DI) provides an accurate framework to describe a wide range of physical systems. It exhibits a rich interplay of short-range nearest-neighbor (NN) exchange interactions and long-range dipole interactions (DI) with nontrivial consequences on systemic properties. The DI pose many challenges in analytical and computational studies. We have performed comprehensive large-scale Monte Carlo (MC) simulations to study the kinetics of domain growth after a temperature quench in the $d = 3$ IM+DI. This phenomenon is interesting for both fundamental and applied studies.

Domain growth in IM+DI is affected by the relative strengths of NN exchange and DI. In the strong dipolar regime, the domains are columnar along the z axis and coarsen faster along z than in the xy plane. At early times, there is transient periodicity of the domains in the xy plane. In general, we find that DI have a profound effect even when they are much weaker than the NN exchange interactions. Columnar morphologies have been observed

experimentally in the dipolar quantum magnet $LiHoF_4$ [31], and ferroelectrics such as rochelle salt, KH_2PO_4, and the technologically important $BaTiO_3$ [9]. The anisotropic growth laws that we observe have not been addressed in experiments. We believe this investigation is important as columnar domains have diverse implications. For example, recent experiments reveal that they are important in the context of electric and magnetic switches in memory devices as they are robust against charge and magnetic field perturbations [35]. Moments in a ferromagnet, on the other hand, can be unintentionally reoriented and the data erased by perturbing magnetic fields generated externally or internally. Further, sidewise motion of domain walls is undesirable to prevent cross-talk between neighboring *electrodes* (columns) on the same crystal plate. In a related context, columnar phases can also be employed in the creation of anisotropic microstructures. The robust morphologies of columns of up spins and down spins in dipolar solids could therefore offer novel experimental possibilities. Laboratory experiments probably access long-lived metastable states, the kind obtained in our simulations. Our numerics can hence be exploited to estimate interfacial energies, barrier energies, and relaxation times of experimental samples. We believe that this work is a starting point to understand pattern formation, morphological features, growth laws, and other nonequilibrium properties in these complex systems.

A.B. and V.B. acknowledge partial financial support from Department of Science and Technology (DST) India, Ministry of Science and Technology, and the HPC facility of IIT Delhi. S.P. is grateful to the DST for support through a J.C. Bose fellowship.

[1] R. Kretschmer and K. Binder, Phys. Rev. B **20**, 1065 (1979).
[2] A. Abragam *et al.*, J. Phys. Colloq. **39**, C6-1436 (1978).
[3] A. Landesman, J. Phys. Colloq. **39**, C6-1305 (1978).
[4] A. Zalkin *et al.*, J. Chem. Phys. **39**, 2881 (1963).
[5] W. P. Wolf *et al.*, J. Appl. Phys. **39**, 1134 (1968).
[6] E. Lagendijk *et al.*, Physica **61**, 220 (1972).
[7] A. A. Molnar *et al.*, Ferroelectrics **192**, 137 (1997).
[8] F. Jona and G. Shirane, *Ferroelectric Crystals* (Pergamon, New York, 1962), Vol. 1.
[9] W. J. Merz, Phys. Rev. **95**, 690 (1954).
[10] A. Biltmo and P. Henelius, Phys. Rev. B **76**, 054423 (2007); Europhys. Lett. **87**, 27007 (2009).
[11] D. Bitko, T. F. Rosenbaum, and G. Aeppli, Phys. Rev. Lett. **77**, 940 (1996).
[12] T. Garel and S. Doniach, Phys. Rev. B **26**, 325 (1982).
[13] J. M. Luttinger and L. Tisza, Phys. Rev. **70**, 954 (1946).
[14] A. Larkin and D. Khmel'nitskii, Sov. Phys. JETP **29**, 1123 (1969).
[15] A. Aharony, Phys. Rev. B **8**, 3363 (1973).
[16] E. Frey and F. Schwabl, Phys. Rev. B **42**, 8261 (1990).
[17] S. Henneberger, E. Frey, P. G. Maier, F. Schwabl, and G. M. Kalvius, Phys. Rev. B **60**, 9630 (1999).
[18] G. Ahlers *et al.*, Phys. Rev. Lett. **34**, 1227 (1975).
[19] R. Frowein, J. Kötzler, and W. Assmus, Phys. Rev. Lett. **42**, 739 (1979).
[20] J. H. Toloza, F. A. Tamarit, and S. A. Cannas, Phys. Rev. B **58**, R8885(R) (1998).
[21] C. Roland and R. C. Desai, Phys. Rev. B **42**, 6658 (1990).
[22] S. Puri and V. Wadhawan, *Kinetics of Phase Transitions* (CRC, Boca Raton, FL, 2009).
[23] L. Ratke and P. W. Voorhees, *Growth and Coarsening: Ostwald Ripening in Material Processing* (Springer-Verlag, Berlin, 2013).
[24] I. M. Lifshitz, Sov. Phys. JETP **15**, 939 (1962).
[25] S. M. Allen and J. W. Cahn, Acta Metall. **27**, 1085 (1979).
[26] J. Villain, Phys. Rev. Lett. **52**, 1543 (1984).
[27] G. P. Shrivastav *et al.*, Europhys. Lett. **96**, 36003 (2011).
[28] A. Bupathy, V. Banerjee, and S. Puri, Phys. Rev. E **93**, 012104 (2016).
[29] F. Corberi, E. Lippiello, A. Mukherjee, S. Puri, and M. Zannetti, Phys. Rev. E **85**, 021141 (2012).
[30] D. Frenkel and B. Smit, *Understanding Molecular Simulations: From Algorithms to Applications* (Academic, San Diego, 1996).
[31] J. E. Battison *et al.*, J. Phys. C **8**, 4089 (1975).
[32] S. Puri, K. Binder, and S. Dattagupta, Phys. Rev. B. **46**, 98 (1992).
[33] S. Puri *et al.*, J. Stat. Phys. **75**, 839 (1994).
[34] A. J. Bray, Phys. Rev. E **47**, 3191 (1993).
[35] P. Wadley *et al.*, Science **351**, 587 (2016).